Bull. Chem. Soc. Ethiop. 1999, 13(2), 155-165.
Printed in Ethiopia

ISSN 1011-3294

n-BUTANE HYDROGENOLYSIS CATALYZED BY ALUMINA-SUPPORTED OSMIUM: PRECURSOR EFFECTS

E.O. Odebunmi

Chemistry Department, University of Ilorin, P.M.B. 1515, Ilorin, Nigeria

(Received July 1, 1999; revised November 29, 1999)

ABSTRACT. The catalytic hydrogenolysis of n-butane by alumina-supported osmium derived from chloroosmic acid (H_2OsCl_6), mononuclear osmium carbonyl ($H_2Os(CO)_4$) and triosmium dodecarbonyl cluster compound ($Os_3(CO)_{12}$) has been studied at a temperature of 130-240 °C and total gas pressure of 1.03 atmosphere. The effect of the osmium precursor on the hydrogenolysis rate and the distribution of products was investigated and appropriate rate equations were used to fit the data. The hydrogenolysis activity of the catalysts was found to be in the decreasing order: 5% Os/Al_2O_3 > 2% $Os_3(CO)_{12}/Al_2O_3$ > 1.66% Os/Al_2O_3. The catalysts also exhibited different partial pressure dependence. The product distribution indicate that whereas ethane was the predominant product on the chloroosmic acid derived 5% Os/Al_2O_3 and the $H_2Os(CO)_4$ derived 1.66% Os/Al_2O_3; it was not the same for the 2% $Os_3(CO)_{12}/Al_2O_3$ where the ethane to methane ratio was 1. These results are explained and attributed to the effect of the osmium precursor used to prepare the catalysts as well as the osmium loading of the catalysts.

INTRODUCTION

Catalytic hydrogenolysis of hydrocarbons is a reductive cleavage of a sigma bond involving the rupture of carbon-carbon bonds via interaction with hydrogen. Following the pioneering work of Taylor and co-workers on hydrogenolysis of simple hydrocarbons [1-3], research efforts have been geared towards the understanding of the mechanisms and kinetics of reaction of hydrocarbon molecules on different supported-metal catalysts [4-11]. Other studies involved structure-activity relationships in hydrogenolysis catalysts [12-15], and the effects of degree of dispersion, crystallite size, metal loading, catalyst pretreatment, reactor start-up procedure as well as metal-support interaction on the hydrogenolysis rates [16-18, 19-25].

The catalytic hydrogenolysts of n-butane presents an interesting study because of the possibility of several products depending upon the reaction conditions and catalysts involved as the scheme below shows:

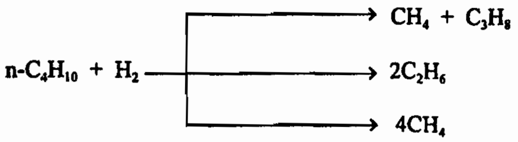

(1)

The kinetic analysis of the above reaction could be complicated because of the possibility of secondary hydrogenolysis of the products. For example, propane formed in the top step could be converted to methane and ethane. Furthermore, the reaction provides an opportunity to study structure-activity relationships of catalysts [4-10, 25].

In earlier communications, we have reported the kinetics and mechanism of hydrogenolysis of ethane and cyclopropane on metal oxide-supported osmium catalysts derived from different osmium precursors [18, 26]. We now present the results of the hydrogenolysis of n-butane over osmium catalysts derived from chloroosmic acid (H_2OsCl_6), the triosmium dodecarbonyl cluster compound ($Os_3(CO)_{12}$) and the mononuclear osmium carbonyl compound ($H_2Os(CO)_4$) as precursors. The aim of the study is to investigate the effects of catalyst precursor and catalyst particle size on the hydrogenolysis rates and the distribution of reaction products. Thus this study is similar to earlier reports on the hydrogenation of carbon monoxide, catalyzed by supported osmium catalysts [11,13,16].

EXPERIMENTAL

Catalyst preparation. The 5% (w/w) Os/Al_2O_3 catalyst derived from chloroosmic acid (H_2OsCl_6) was prepared by the method of aqueous impregnation. This involved dissolving appropriate quantity of H_2OsCl_6 (Colonial Metals, USA) in deionized water and mixing the solution with the gamma alumina (Ketjen, 240 m^2/g) support to form a wet paste which was subsequently dried at 110 °C under nitrogen. The dried sample was then ground into a fine powder and reduced in flowing hydrogen gas (Table 1) in the reactor before use in a catalytic reaction experiment [11,18].

The 2 % (w/w) $Os_3(CO)_{12}/Al_2O_3$ catalyst was prepared by refluxing a solution of $Os_3(CO)_{12}$ in n-heptane with the gamma alumina support as described previously [11, 27]. The 1.66% (w/w) $H_2Os(CO)_4/Al_2O_3$ catalyst was made by adding appropriate quantity of calcined gamma alumina to the $H_2Os(CO)_4$ solution (Strem, USA) in n-hexane. The solid was then separated from the solution and was dried in flowing nitrogen and then under vacuum.

Catalyst pretreatment preceded each kinetic run and usually involved flushing with helium for 15 minutes, heating in flowing helium from room temperature to 240 °C, and then keeping helium flowing over the catalyst at this temperature for 8 hours. This procedure was followed for the pretreatment of all the three catalysts (Table 1).

Table 1. Alumina-supported osmium catalysts for n-butane hydrogenolysis: catalyst pretreatment[a] and reaction conditions.

Catalyst precursor/support[c]	Osmium content % (w/w)	Reaction conditions[b]				
		Temp °C	Feed composition (% mol)			
			C_4	H_2	Helium	H_2/C_4 ratio
H_2OsCl_6/Al_2O_3	5	130-190	5.0	45	50	9
$Os_3(CO)_{12}/Al_2O_3$	2	150-240	4.5	36.8	58.7	8
$H_2Os(CO)_4/Al_2O_3$	1.66	200-240	5.0	45	50	9

[a] Catalyst pretreatment involved heating in helium at reaction temprature for several hours.The chloroosmic acid-derived catalyst was reduced in hydrogen gas at 240 °C for 10 hours while the osmium carbonyl derived were reduced in hydrogen gas at 240 °C for one hour [11]. [b] Total pressure = 1.03 atm for all the experiments. [c] These catalysts have previously been characterised by H_2 and CO chemisorption, FTIR and TEM measurements [11].

Catalytic reaction rate measurements. The catalytic hydrogenolysis of n-butane was studied in a low pressure flow reactor system interfaced with an Antek Gas-Chromatograph (GC) equipped with a flame ionization detector and a 1/8" x 6' stainless steel column packed with activated alumina [18, 27]. The reactor, a pipette-shaped Pyrex glass tube, was filled with varying amounts of catalyst particles which were held in place by plugs of calcined glass-wool at inlet and outlet.

Following catalyst pretreatment, the n-butane hydrogenolysis reaction was initiated by contacting the catalyst with the reactant gases at a presure of 1.03 atmosphere and other conditions as indicated in Table 1. For all the experiments, the hydrogen to n-butane mole ratio was 8 or 9. The effluent from the reactor was carried into a sampling valve attached to the Antek GC through heated lines. The GC column conditions involved an initial 1 min hold at 40 °C, temperature programming at 8 °C/min to 110 °C, and then a final 1 min hold at 110 °C. This ensured efficient separation of the components of the reactant and reaction product samples. The GC was calibrated with a calibration gas (containing 0.951% methane, 0.996% ethane, 0.998% propane, and 0.999% n-butane with helium making up the balance) to determine response factors and retention times for compounds. Products were identified by their retention times. Other details of the apparatus and procedures have been given elsewhere [18]. Blank experiments showed that the alumina support had no catalytic activity at 240 °C and 1.03 atmosphere total pressure.

The initial rates were calculated by using the equation:

$$r = X . (F/W) \tag{2}$$

where X = fractional conversion, F = moles of feed per second, and W = amount of catalyst (g) in the reactor.

RESULTS AND DISCUSSION

Performance of the 5% Os/Al_2O_3 prepared from chloroosmic acid (H_2OsCl_6). The experiments were carried out and kinetic data were collected at temperatures of 130-191 °C, total gas pressure of 1.03 atmosphere with a feed composition of 5 mol% n-butane, 45 mol% hydrogen and 50 mol% helium (i.e. with hydrogen to n-butane, mole ratio of 9). The percent conversion of n-butane to ethane as a function of the reciprocal space velocity (Figure 1) showed that the reaction was in the differential conversion regime up to 161 °C. A similar plot was obtained for the conversion of n-butane to methane. The curvature of the plot at 191°C (the highest temperature

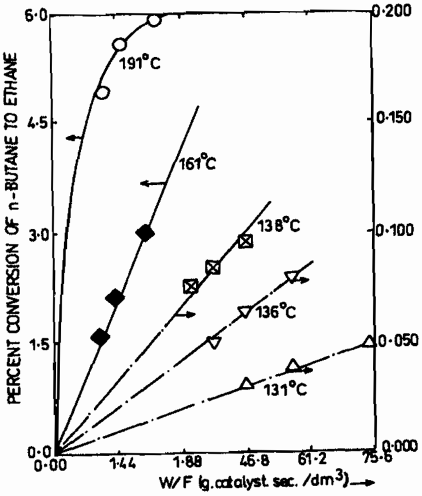

Figure 1. Conversion *vs* W/F for ethane formation on 5% $Os/\gamma\text{-}Al_2O_3$.

of this study) indicates that the temperature was too high for the conversion. In this case therefore the initial reaction rate was determined by extrapolating the slope of conversion versus reciprocal space velocity to the origin.

The Arrhenius plots for methane and ethane formation were linear and the apparent activation energies (E) were calculated to be 224 and 201 kJ/mol for methane and ethane formation, respectively. The correlation coefficients of the Arrhenius plots are 0.995 and 0.997 for methane and ethane formation, respectively.

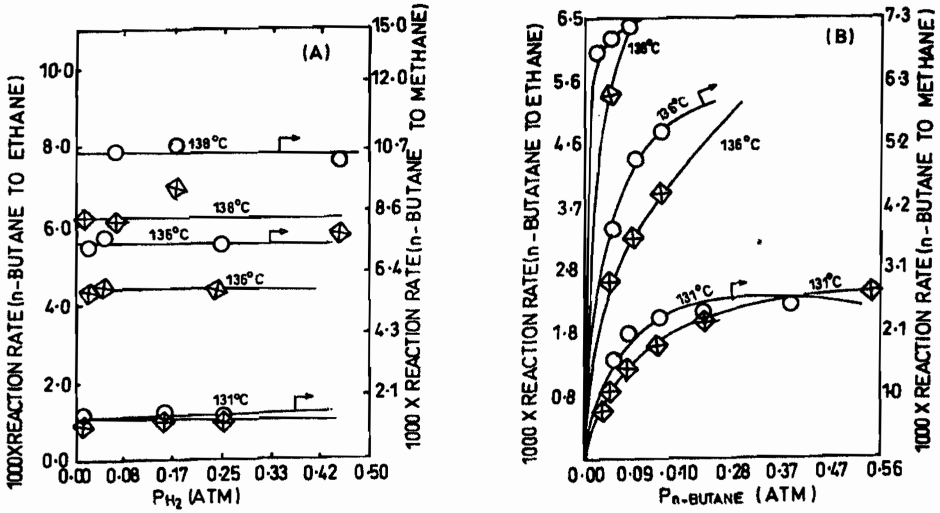

Figure 2. Reaction rate *versus* partial pressure of (A) hydrogen and (B) n-butane for ethane and methane formation on 5% Os/γ-Al_2O_3.

The dependence of the initial rate of hydrogenolysis on the partial pressure of hydrogen was investigated by measuring the initial rate at a constant partial pressure of n-butane while varying the partial pressure of hydrogen from 0.05 to 0.50 atmosphere. The dependence of the rate on the partial pressure of n-butane was determined by measuring the initial rate at constant hydrogen partial pressure of 0.45 atmosphere while varying the partial pressure of n-butane in the range of 0.02 to 0.57 atmosphere and at a total pressure of 1.03 atmosphere. The results are presented as Figures 2A and 2B. The initial rates were found to be independent of the hydrogen partial pressure (Figure 2A) but were strongly dependent on the partial pressure of n-butane (Figure 2B) at all the temperatures investigated. The same results were obtained for methane and ethane formation.

The final expression of the initial rates were determined with experiments at a constant hydrogen partial pressure of 0.45 atm and n-butane partial pressure in the range of 0.02 to 0.57 atm. The data were fitted by a Langmuir-Hinshelwood-Hougen-Watson reaction rate expression for methane and ethane formation of the form [28, 29]:

$$r = \frac{kP_B}{(1 + KP_B)} \tag{3}$$

The apparent rate constants were determined by plotting reciprocal initial reaction rate *versus* reciprocal partial pressure of n-butane (Figure 3) for methane and ethane formation, respectively.

The results are given in Table 2. For this catalyst (5% Os/Al_2O_3) propane was observed as a product only at 191°C.

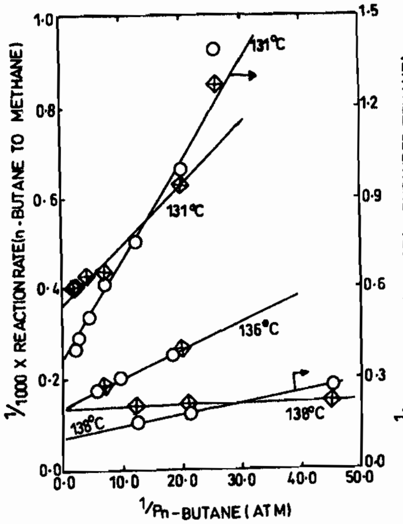

Figure 3. Determination of rate constants for methane and ethane formation on 5% $Os/\gamma\text{-}Al_2O_3$.

Performance of the 2% $Os_3(CO)_{12}/Al_2O_3$ prepared from $Os_3(CO)_{12}$. Experimental data were collected under the reaction conditions given in Table 1. The results of preliminary experiments at higher temperatures showed that the reaction was inhibited greatly when conversion of butane was greater than 14%. Thus low temperatures were used in order to investigate the reaction kinetics under differential conversion conditions. The plot of the percent conversion of n-butane to methane versus reciprocal space velocity is given in Figure 4. High correlation coefficient of 0.998 was obtained for each line. Similar results were obtained for conversion to ethane and propane. The Arrhenius plots for methane formation were linear with high correlation coefficients. The apparent activation energy for methane formation was found to be 39 kJ/mol.

In order to clarify the reaction kinetics, initial rates were measured as the partial pressures of hydrogen and n-butane were changed individually at a total pressure of 1.03 atmosphere. The results are given in Figure 5. The reaction rate was found to be independent of the partial pressure of n-butane from 0.024 to 0.12 atm, but the rate depended strongly on the partial pressure of hydrogen (Figure 5). When the partial pressure of hydrogen was varied from 0.05 to 0.44 atm at a constant n-butane partial pressure of 0.05 atm, the data fitted the following Langmuir-Hinshelwood-Hougen-Watson rate expression for methane formation.

$$r = \frac{kP_H}{(1 + KP_H)} \tag{4}$$

Using this equation the apparent initial reaction rate constants were determined from a double reciprocal plot of reaction rate against hydrogen partial pressure. The results are given in Figure 6 and Table 2.

Table 2. Rate equations and apparent kinetic parameters for n-butane hydrogenolysis on osmium/alumina catalysts.

Catalyst	Rate equation	T °C	10^3k mol.g^{-1} hr^{-1}	K Atm^{-1}	E kJ/mol	Product distribution Main product	 C2/C1	 C3 formed
I 5% Os/Al_2O_3	$\boxed{\frac{kP_B}{(1+KP_B)}}$	*Ethane Formation*						
		131	0.03	8.38				
		136	1.0	20.10	201[a]	Ethane	3.1	Yes
		138	2.7	30.27				
		Methane Formation						
		131	0.006	19.31				
		136	0.02	210.91	22[b]			
		138	0.33	456.67				
II 2% $Os_3(CO)_{12}/Al_2O_3$	$\boxed{\frac{kP_H}{(1+KP_H)}}$	191	4.3	3.53	39[a]	Methane	1.0	Yes
III $1.66\%H_2O_3(CO)_4/Al_2O_3$	*Model I* $\boxed{\frac{k\,P_B P_H}{(1+KP_H)}}$	240	780.53	8.36	113[a]	Ethane	3.1	No
	Model II $\boxed{\frac{kP_B P_H}{(1+KP_H)^2}}$	240	624.99	2.21	129[b]			

[a]For ethane formation. [b]For methane formation.

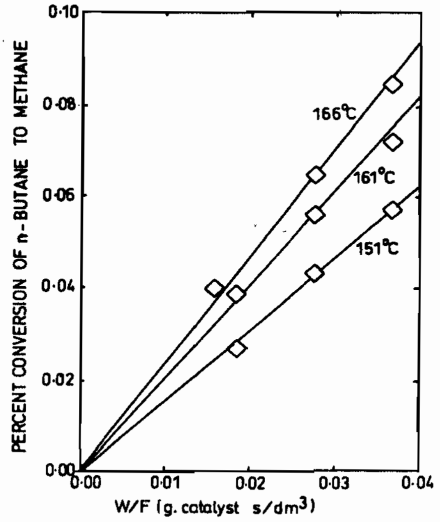

Figure 4. Conversion *vs* W/F for methane formation on 2% $Os_3(CO)_{12}/\gamma\text{-}Al_2O_3$.

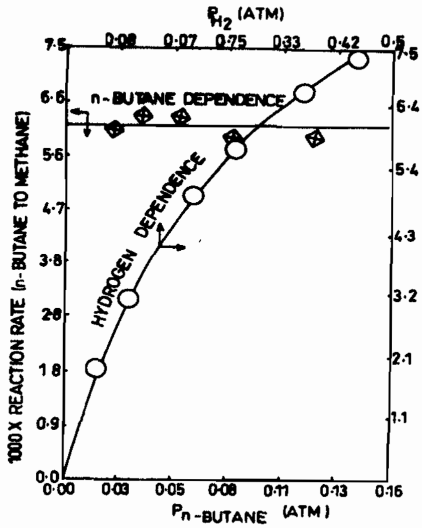

Figure 5. Reaction rate *vs* partial pressure of n-butane and hydrogen for methane formation on 2% $Os_3(CO)_{12}/\gamma\text{-}Al_2O_3$ at 191 °C.

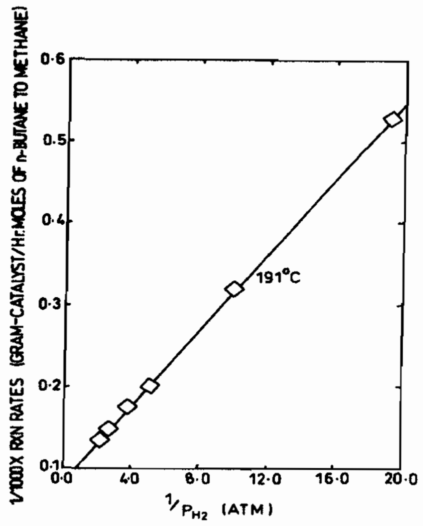

Figure 6. Determination of rate constants for methane formation on 2% $Os_3(CO)_{12}/\gamma\text{-}Al_2O_3$.

Performance of the 1.66% Os/Al_2O_3 prepared from $H_2Os(CO)_4$. For this catalyst experimental data were collected with a feed composition of 5 mol % n-butane 45 mol % hydrogen and 50 mol % helium, temperature of 201-240 °C and with a total gas pressure of 1.03 atmosphere. As with other catalysts, plots of conversion as a function of the reciprocal space velocity were linear with high correlation coefficients of 0.998 for both methane and ethane formation. No propane was produced. The conversion ratio of n-butane converted to ethane to that converted to methane was 3.14 (Table 2). The data show that the reaction was operated in the differential conversion regime so that reaction rates were independent of contact time. Apparent activation energies were calculated from linear Arrhenius plots and found to be 129 and 113 kJ/mole for methane and ethane formation, respectively.

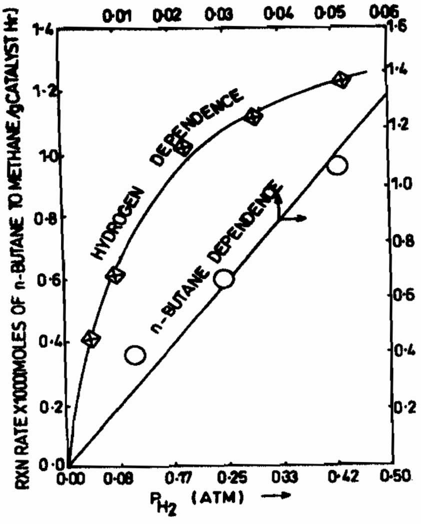

Figure 7. Reaction rate *vs* partial pressure of hydrogen and n-butane for methane formation on 1.66%Os/γ-Al_2O_3 at 240 °C.

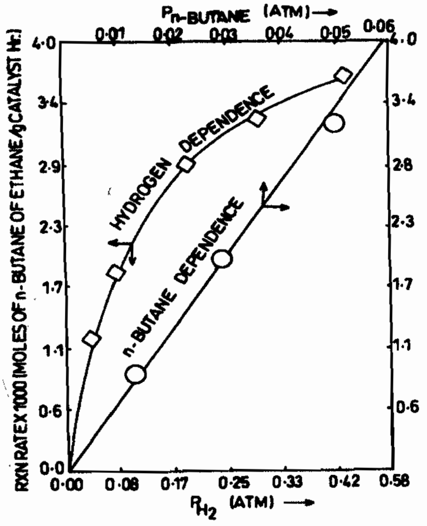

Figure 8. Reaction rate *vs* partial pressure of hydrogen and n-butane for ethane formation on 1.66% Os/γ-Al_2O_3 at 240 °C.

To determine the order of reaction the hydrogen partial pressure was varied from 0.043 to 0.44 atmosphere and at a constant n-butane pressure of 0.05 atmosphere and constant temperature of 240 °C. The order of reaction in n-butane was determined with experiments at a constant hydrogen partial pressure of 0.45 atmosphere. The results (Figures 7 and 8) show that the reaction was first order in n-butane for both the methane and ethane formation. However the reaction was inhibited by hydrogen and a Langmuir-Hinshelwood-Hougen-Watson kinetic model was used to fit the data. The full kinetics are represented by an equation of the form:

$$r = \frac{kP_BP_H}{(1 + KP_H)} \tag{5}$$

for both methane and ethane formation. The parameters in the reaction equation were determined by using a non-linear regression programme to fit the data. The results are presented in Table 2 for the different kinetic models tried.

Comparison of the catalysts

(a) Relative catalytic activity. All the three alumina-supported osmium catalysts were active for the hydrogenolysis of n-butane. They exhibited different activities with the 5% Os/Al_2O_3 derived from H_2OsCl_6 being the most active while the 1.66% Os/Al_2O_3 derived from $H_2Os(CO)_4$ the least active. The activity of the 2% $Os_3(CO)_{12}/Al_2O_3$ catalyst is intermediate between these two. Since the activities of the three catalysts are very different the temperature range required to maintain differential conversion for each catalyst did not overlap (Table 1). The differences in the catalytic activities of the three osmium catalysts would have been greater than observed if chemisorption studies had been done and reaction rates were reported as moles of product formed per second per catalyst site.

The relative activity observed is similar to what was reported earlier for the hydrogenation of carbon monoxide catalyzed by supported osmium [11]. The catalytic activity for hydrocarbon formation was found to increase with increasing osmium aggregate size. The chloroosmic acid-derived catalyst with large particles of osmium (70 Å) had the highest activity, while the triosmium dodecarbonyl ($Os(CO)_{12}$) derived catalyst (10-20 Å) had the lowest activity. The approximate average particle size was determined by transmission electron microscopy (TEM) [11]. The hydrogenolysis reaction is in a sense the reverse reaction of the hydrocarbon synthesis reaction. Thus it is not very surprising that the factor that affects the synthesis reaction is affecting the hydrogenolysis reaction also. Furthermore, in the present study, the catalytic activity for n-butane hydrogenolysis appears to increase also with increasing osmium content (osmium loading) of the catalyst. Thus the osmium loading appears to affect the aggregate size which in turn affects the hydrogenolysis activity.

(b) Pressure dependence of reaction rate. The three alumina-supported osmium catalysts not only exhibited different hydrogenolysis activities, but also different partial pressure dependence. For the triosonium carbonyl cluster-derived catalyst, the reaction rate was found to be independent of the partial-pressure of n-butane (equation 4), and this behaviour is totally different from the results obtained with the other two catalysts (equations 3 and 5). The partial pressure dependence of the n-butane hydrogenolysis rate for the other two catalysts are in agreement with literature reports [9, 30]. Furthermore, the apparent rate equation for the 5% Os/Al_2O_3 catalyst agrées with that observed for rhenium and ruthenium [31, 32], and the one for the 1.66 % Os/Al_2O_3 agrees with the result obtained for ruthenium catalyst [19].

For the metallic osmium catalyst (i.e. 5% Os/Al_2O_3) the lack of dependence of the hydrogenolysis rate on hydrogen partial pressure differs significantly from the results of previous studies [16, 25]. In general, the dependence of the n-butane hydrogenolysis rate on the partial pressure of hydrogen has been found to vary from positive to zero and then to negative order in hydrogen with increasing partial pressure of hydrogen. Thus our results for metallic osmium are in the zero range of the hydrogen order. This is probably due to the fact that metallic osmium strongly adsorbs hydrogen, so that the rate determining step is the adsorption of n-butane on metallic osmium surface as required by the apparent rate expression which fits the data best (equation 3).

(c) Product distribution and reaction mechanism. The product distributions for the three catalysts are compared in Table 2. The data show that ethane was the main product of n-butane hydrogenolysis for the catalysts derived from chloroosmic acid and the mononuclear osmium carbonyl while methane was the main product for the catalyst derived from the triosmium carbonyl cluster compound. The behaviour of the triosmium carbonyl compound is similar to what was reported for the rhenium catalyst [9]. On the other hand, the product distribution in terms of formation of methane and ethane observed for the other two catalysts agrees with several literature reports [10, 20, 25].

The data in Table 2 show further that whereas propane was formed in the hydrogenolysis reaction involving 5% Os/Al_2O_3 and 2% $Os_3(CO)_{12}/Al_2O_3$ catalysts, it was not observed with the 1.66% Os/Al_2O_3 catalyst. These observations as well as the widely different values of the activation energies and other kinetic parameters for the three catalysts (Table 2) show clearly that the reaction mechanism are different for the three catalysts, as the rate equations already show.

The present experimental data are however not adequate to pursue this further. In an earlier communication [11], we have demonstrated that the alumina-supported osmium catalysts derived from different osmium compounds exhibited different catalytic behaviour for carbon monoxide hydrogenation. This was confirmed by the results of characterization by infrared spectroscopy (FTIR) and high resolution transmission electron microscopy (TEM) [11, 13, 27]. The present results agree with the above and indicate that the catalyst precursor strongly influences the catalytic behaviour, product distribution and reaction mechanisms for the hydrogenolysis of n-butane by alumina-supported osmium catalysts.

REFERENCES

1. Morikawa, K; Benedict, W.S; Taylor, H.S. *J. Am. Chem. Soc.* **1936**, 58, 1795.
2. Taylor, E.H; Taylor, H.S. *J. Am. Chem. Soc.* **1939**, 61, 503.
3. Kemball, C.; Taylor, H.S. *J. Am. Chem. Soc.* **1948**, 20, 345.
4. Hung-Chung, W.; Li-jen, L.; Claude, N.; Knei-jung, C. *J. Mol. Catal. A: Chemical* **1997**, 127, 143.
5. Fogash, K.B; Hong, Z.; Dumesic, J.A. *J. Catal.* **1998**, 173, 519.
6. Barkova, A.P.; Furman, D.B. *Kinetics and Catalysis* **1998**, 39, 137.
7. Ihi, H.C.; Seung, B.P.; Sung, J.C.; Ryong, R. *J. Catal.* **1998**, 173, 295.
8. Bond, G.C.; Xu, Y. *J. Chem. Soc. Faraday. Trans. I* **1984**, 80, 969.
9. Sinfelt, J.H. *Catal. Rev. Sci. Eng.* **1969**, 3, 175.
10. Leclerq, G; Leclerq, L; Bouleau, L.M; Pietry, K.S.; Mannel, R. *J. Catal.* **1984**, 88, 8.
11. Odebunmi, E.O.; Matrana, B.A; Datye, A.K; Allard, Schwank J; Manogue, W.H; Hayman, A; Onuferko, J.H; Knozinger, H; Gates, B.C. *J. Catal.* **1985**, 95, 370.

12. Gudkov, B.S; Guczi, L.; Tetenyi, P. *J. Catal.* **1982**, 74, 207.
13. Jackson, S.D.; Moyes, R.B; Wells, P.B.; Wyman, P. *J. Catal.* **1984**, 86, 342.
14. Kristyan, S.C.; Szamosi, J.L. *J. Chem. Soc. Faraday Trans. I* **1984**, 80, 1645.
15. Yates, D.J.C.; Taylor, W.F.; Sinfelt, J.H. *J. Am. Chem. Soc.* **1964**, 86, 2996.
16. Leclerq, G; Pietrzyk, S; Peyrovi, M.; Karrona, M. *J. Catal.* **1986**, 99, 1.
17. Yates D.J.C.; Taylor, W.F.; Sinfelt, J.H. *J. Phys. Chem.* **1965**, 69, 95.
18. Odebunmi, E.O. *Bull. Chem. Soc. Ethiop.* **1993**, 7, 43.
19. Kempling, J. *Ind. Eng. Chem. Process. Res. Dev.* **1972**, 11, 1.
20. Bond, G.C.; Newham J. *Faraday Soc. Trans.* **1960**, 56, 1501.
21. Sinfelt, J.H. *J. Phys. Chem.* **1966**, 70, 2257.
22. Kerpinski, Z.; Chuag, T.K.; Katsuzawa, H; Butt, J.B; Burwell Jr., R.L.; Cohen, J.B. *J. Catal.* **1986**, 99, 184.
23. Monnier, J.; Anderson, P. *J. Catal.* **1982**, 78, 419.
24. Cimino, A.; Boudart, M.; Taylor, H.S. *J. Phys. Chem.* **1954**, 58, 796.
25. Bond, G.C.; Lou, H. *J. Catal.* **1993**, 142, 512.
26. Odebunmi, E.O. *Bull. Chem. Soc. Ethiop.* **1996**, 10, 145.
27. Knozinger, H; Zhao, Y; Barth, R; Epstein, R; Gates, B.C.; Scott, J.P. *Faraday Discuss. Chem. Soc.* **1981**, 72, 53.
28. Carberry, J.J. *Chemical and Catalytic Reaction Engineering*, McGraw-Hill Book Company: New York; 1976; p 383.
29. Levenspiel, O. *Chemical Reaction Engineering*, 2nd ed., John Wiley: New York; 1972; p 460.
30. Sinfelt, J.H. *Adv. Catal.* **1973**, 23, 91.
31. Nezimek, D. *React. Kinet. Catal. Lett.* **1980**, 13, 331.
32. Nezimek, D. *React. Kinet. Catal. Lett.* **1985**, 27, 273.